Liquid polyamorphism: Possible relation to the anomalous behaviour of water

H.E. Stanley[1,a], P. Kumar[1], G. Franzese[2], L. Xu[1], Z. Yan[1], M.G. Mazza[1], S.V. Buldyrev[13], S.-H. Chen[4], and F. Mallamace[5]

[1] Center for Polymer Studies and Dept. of Physics, Boston University, Boston, MA 02215, USA
[2] Departament de Física Fonamental, Univ. de Barcelona, Diagonal 647, Barcelona 08028, Spain
[3] Department of Physics, Yeshiva University, 500 West 185th Street, New York, NY 10033, USA
[4] Nuclear Science and Engineering Dept., Mass. Inst. of Technology, Cambridge, MA 02139, USA
[5] Dipartimento di Fisica, Univ. Messina, Vill. S. Agata, CP 55, 98166 Messina, Italy

Abstract. We present evidence from experiments and computer simulations supporting the hypothesis that water displays polyamorphism, i.e., water separates into two distinct liquid phases. This concept of a new liquid-liquid phase transition is finding application to other liquids as well as water, such as silicon and silica. Specifically, we investigate, the relation between changes in dynamic and thermodynamic anomalies arising from the presence of the liquid-liquid critical point in (i) Two models of water, TIP5P and ST2, which display a first order liquid-liquid phase transition at low temperatures; (ii) the Jagla model, a spherically symmetric two-scale potential known to possess a liquid-liquid critical point, in which the competition between two liquid structures is generated by repulsive and attractive ramp interactions; and (iii) A Hamiltonian model of water where the idea of two length/energy scales is built in. This model also displays a first order liquid-liquid phase transition at low temperatures besides the first order liquid-gas phase transition at high temperatures. We find a correlation between the dynamic fragility crossover and the locus of specific heat maxima $C_P^{\max}$ ("Widom line") emanating from the critical point. Our findings are consistent with a possible relation between the previously hypothesised liquid-liquid phase transition and the transition in the dynamics recently observed in neutron scattering experiments on confined water. More generally, we argue that this connection between $C_P^{\max}$ and the dynamic crossover is not limited to the case of water, a hydrogen bonded network liquid, but is a more general feature of crossing the Widom line, an extension of the first-order coexistence line in the supercritical region.

Dedicated to Armin Bunde on the occasion of his 60th birthday.

1 Background

One "mysterious" property of liquid water was recognised 300 years ago [1]: although most liquids contract as temperature decreases, liquid bulk water begins to expand when its temperature drops below 4°C. Indeed, a simple kitchen experiment demonstrates that the bottom layer of a glass of unstirred iced water remains at 4°C while colder layers of 0°C water "float" on top (cf., Fig. 1 of Ref. [2]). The mysterious properties of liquid bulk water become more pronounced in the supercooled region below 0°C [3–5]. For example, if the coefficient of thermal expansion

---

[a] e-mail: `hes@bu.edu`

α_P, isothermal compressibility K_T, and constant-pressure specific heat C_P are extrapolated below the lowest temperatures measurable they would become infinite at a temperature of $T_s \approx 228$ K [3,6].

Water is a liquid, but glassy water—also called amorphous ice—can exist when the temperature drops below the glass transition temperature T_g. Although it is a solid, its structure exhibits a disordered molecular liquid-like arrangement. *Low-density* amorphous ice (LDA) has been known for 60 years [7], and a second kind of amorphous ice, *high-density* amorphous ice (HDA) was discovered in 1984 [8–10]. HDA has a structure similar to that of high-pressure liquid water, suggesting that HDA may be a glassy form of high-pressure water [11,12], just as LDA may be a glassy form of low-pressure water. Water has at least two different amorphous solid forms, a phenomenon called *polyamorphism* [13–19], and recently additional forms of glassy water have been the focus of active experimental and computational investigation [20–28].

1.1 Current hypotheses

Many classic "explanations" for the mysterious behaviour of liquid bulk water have been developed [29–34], including a simple two-state model dating back to Röntgen [35] and a clathrate model dating back to Pauling [36]. Three hypotheses are under current discussion:

(i)   The *stability limit hypothesis* [37], which assumes that the spinodal temperature line $T_s(P)$ between two liquids with different densities in the pressure-temperature $(P - T)$ phase diagram connects at negative P to the locus of the liquid-to-gas spinodal for superheated bulk water. Liquid water cannot exist when cooled or stretched beyond the line $T_s(P)$.

(ii) The *singularity-free hypothesis* [38], considers the possibility that the observed polyamorphic changes in water resemble a genuine transition, but is not. For example, if water is a locally-structured transient gel comprised of molecules held together by hydrogen bonds whose number increases as temperature decreases [39–41], then the local "patches" or bonded sub-domains [42,43] lead to enhanced fluctuations of specific volume and entropy and negative cross-correlations of volume and entropy whose anomalies closely match those observed experimentally.

(iii) The *liquid-liquid (LL) phase transition hypothesis* [44] arose from MD studies on the structure and equation of state of supercooled bulk water and has received some support [45–53]. Below the hypothesised *second* critical point the liquid phase separates into two distinct liquid phases: a low-density liquid (LDL) phase at low pressures and a high-density liquid (HDL) at high pressure (Fig. 1). Bulk water near the known critical point at 647 K is a fluctuating mixture of molecules whose local structures resemble the liquid and gas phases. Similarly, bulk water near the hypothesised LL critical point is a fluctuating mixture of molecules whose local structures resemble the two phases, LDL and HDL. These enhanced fluctuations influence the properties of liquid bulk water, thereby leading to anomalous behaviour.

1.2 Selected experimental results

Many precise experiments have been performed to test the various hypotheses discussed in the previous section, but there is as yet no widespread agreement on which physical picture—if any—is correct. The connection between liquid water and the two amorphous ices predicted by the LL phase transition hypothesis is difficult to prove experimentally because super-cooled water freezes spontaneously below the homogeneous nucleation temperature T_H, and amorphous ice crystallises above the crystallisation temperature T_X [54–56]. Crystallisation makes experimentation on the supercooled liquid state between T_H and T_X almost impossible. However, comparing experimental data on amorphous ice at low temperatures with that of liquid water at higher temperatures allows an indirect discussion of the relationship between the liquid and amorphous states. It is found from neutron diffraction studies [12] and simulations that the structure of liquid water changes toward the LDA structure when the liquid is cooled

at low pressures and changes toward the HDA structure when cooled at high pressures, which is consistent with the LL phase transition hypothesis [12]. The amorphous states (LDA and HDA) are presently considered to be "smoothly" connected thermodynamically to the liquid state if the entropies of the amorphous states are small [57,58], and experimental results suggest that their entropies are indeed small [59].

In principle, it is possible to investigate experimentally the liquid state in the region between T_H and T_X during the extremely short time interval before the liquid freezes to crystalline ice [17,56,60]. Because high-temperature liquid bulk water becomes LDA without crystallisation when it is cooled rapidly at one bar [16,61], LDA appears directly related to liquid water. A possible connection between liquid bulk water at high pressure and HDA can be seen when ice crystals are melted using pressure [17]. Other experimental results [56] on the high-pressure ices [34,62] that might demonstrate a LL first-order transition in the region between T_H and T_X have been obtained.

1.3 Selected results from simulations

Water is challenging to simulate because it is a molecular liquid and there is presently no precise yet tractable intermolecular potential that is universally agreed on. Nevertheless there are some distinct advantages of simulations over experiments. Experiments cannot probe the "No-Man's land" that arises in bulk water from homogeneous nucleation phenomena, but simulations have the advantage that they can probe the structure and dynamics well below T_H since nucleation does not occur on the time scale of computer simulations. Of the three hypotheses above, the LL phase transition hypothesis is best supported by simulations, some using the ST2 potential which *exaggerates* the real properties of bulk water, and others using the SPC/E and TIP4P potentials which *underestimate* them [44,63–67]. Recently, simulations have begun to appear using the more reliable TIP5P potential [68–70]. The precise location of the LL critical point is difficult to obtain since the continuation of the first order line is a locus of maximum compressibility [63,64,66].

Further, computer simulations may be used to probe the *local* structure of water. At low temperatures, many water molecules appear to possess one of two principal local structures, one resembling LDA and the other HDA [44,63,65,71]. Experimental data can also be interpreted in terms of two distinct local structures [72–74].

2 Understanding "static heterogeneities"

The systems in which water is confined are diverse—including the rapidly-developing field of artificial "nanofluidic" systems (man-made devices of order of nanometer or less that convey fluids). Among the special reasons for our interest in confined water is that phenomena occurring at a given set of conditions in bulk water occur under perturbed conditions for confined water [75–88]. For example, the coordinates of the hypothesised LL critical point lie in the experimentally-inaccessible No-Man's land of the bulk water phase digram, but appear to lie in an accessible region of the phase diagrams of both two-dimensionally and one-dimensionally confined water [89,90]. Simulations have been carried out to understand the effect of purely geometrical confinement [91–96] and of the interaction with hydrophilic [97–101] or hydrophobic [102–105] surfaces. It is interesting also to study the effects that confinement may have on the phase transition properties of supercooled water [96], in order to clarify the possible presence of a LL phase transition in the water. Recent work on the phase behaviour of confined water suggests a sensitive dependence on the interaction with the surfaces [104], as a LL phase transition appears to be consistent with simulations of water confined between two parallel flat hydrophobic walls [94]. Works are in progress to extend this work to hydrophilic pores, such as those in Vycor glasses or biological situations, and to hydrophobic hydrogels, systems of current experimental interest [94,106–121].
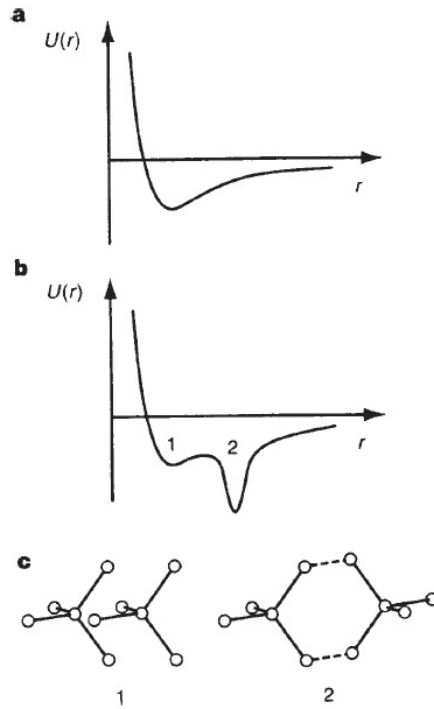
Fig. 1. (a) Idealised system characterised by a pair interaction potential with a single attractive well. At low enough T ($T < T_C$) and high enough P ($P > P_C$), the system condenses into the "liquid" well shown. (b) Idealised system characterised by a pair interaction potential whose attractive well has two sub-wells, the outer of which is deeper and narrower. For low enough T ($T < T_{c'}$) and low enough P ($P < P_{c'}$), the one-phase liquid can "condense" into the narrow outer "LDL" sub-well, thereby giving rise to a LDL phase, and leaving behind the high-density liquid phase occupying predominantly the inner subwell. (c) Two idealised interaction clusters of water molecules in configurations that may correspond to the two sub-wells of (b).

2.1 Potentials with two characteristic length scales: Physical arguments

A critical point appears if the pair potential between two particles of the system exhibits a minimum, and Fig. 1(a) sketches the potential of such an idealised system. At high temperature, the system's kinetic energy is so large that the potential well does not have an effect, and the system is in a single "fluid" (or gas) phase. At low enough temperature ($T < T_C$) and large enough pressure ($P > P_C$) the fluid is sufficiently influenced by the minimum in the pair potential that it can condense into the low specific volume liquid phase. At lower pressure ($P < P_C$), the system explores the full range of distances—the large specific volume gas phase.

If the potential well has the form shown in Fig. 1(b)—the attractive potential well of Fig. 1(a) has now bifurcated into a deeper outer sub-well and a more shallow inner sub-well. Such a two-minimum ("two length scale") potential can give rise to the occurrence at low temperatures of a LL critical point at $(T_{C'}, P_{C'})$ [122]. At high temperature, the system's kinetic energy is so large that the two sub-wells have no appreciable effect on the thermodynamics and the liquid phase can sample both sub-wells. However, at low enough temperature ($T < T_{C'}$) and not too high a pressure ($P < P_{C'}$) the system must respect the depth of the outer sub-well so the liquid phase "condenses" into the outer sub-well (the LDL phase). At higher pressure it is forced into the shallower inner sub-well (the HDL phase).

The above arguments concern the average or "thermodynamic" properties, but they may also be useful in anticipating the local properties in the neighbourhood of individual molecules [123]. Consider, again, an idealised fluid with a potential of the form of Fig. 1(a), and suppose that T is, say, 1.2 T_C so that the macroscopic liquid phase has not yet condensed out. Although

the system is not entirely in the liquid state, small clusters of molecules begin to coalesce into the potential well, thereby changing their characteristic interparticle spacing (and hence their local specific volume) and their local entropy, so the fluid system will experience spatial fluctuations characteristic of the liquid phase even though this phase has not yet condensed out of the fluid at $T = 1.2 \ T_C$. Specific volume fluctuations are measured by the isothermal compressibility and entropy fluctuations by the constant-pressure specific heat, so these two functions should start to increase from the values they would have if there were no potential well at all. As T decreases toward T_C, the magnitude of the fluctuations (and hence of the compressibility and the specific heat) increases monotonically and in fact diverges to infinity as $T \to T_C$. The cross-fluctuations of specific volume and entropy are proportional to the coefficient of thermal expansion, and this (positive) function should increase without limit as $T \to T_C$.

Consider an idealised fluid with a potential of the form of Fig. 1(b), and suppose that T is now *below* T_C but is 20 percent *above* $T_{C'}$, so that the LDL phase has not yet condensed out. The liquid can nonetheless begin to sample the two sub-wells and clusters of molecules will begin to coalesce in each well, with the result that the liquid will experience spatial fluctuations characteristic of the LDL and HDL phase even though the liquid has not yet phase separated. The specific volume fluctuations and entropy fluctuations will increase, and so the isothermal compressibility K_T and constant-pressure specific heat C_P begin to diverge. Moreover, if the outer well is narrow, then when a cluster of neighboring particles samples the outer well it has a larger specific volume and a smaller entropy, so the anticorrelated cross-fluctuations of specific volume (the isothermal expansion coefficient α_P) is now *negative*, and approaching $-\infty$ as T decreases toward $T_{C'}$.

Now if by chance the value of $T_{C'}$ is lower than the value of T_H, then the phase separation discussed above would occur only at temperatures so low that the liquid would have frozen! In this case, the "hint" of the LL critical point C' is the presence of these local fluctuations whose magnitude would grow as T decreases, but which would never actually diverge if the point C' is never actually reached. Functions would be observed experimentally to increase as if they would diverge to ∞ or $-\infty$ but at a temperature below the range of experimental accessibility.

Now consider not the above simplified potential, but rather the complex (and unknown) potential between nonlinear water molecules. The tetrahedrality of water dictates that the outermost well corresponds to the ordered configuration with lower entropy. Thus although we do not know the actual form of the intermolecular potential in bulk water, it is not implausible that the same considerations apply as those discussed for the simplified potential of Fig. 1(b). Indeed, extensive studies of such pair potentials have been carried out recently and the existence of the LL critical point has been demonstrated in such models [47, 48, 50–53, 124, 125, 143–147].

To make more concrete how plausible it is to obtain a bifurcated potential well of the form of Fig. 1(b), consider that one can crudely approximate water as a collection of 5-molecule groups called Walrafen pentamers (Fig. 1(c)) [73]. The interaction strengths of two adjacent Walrafen pentamers depends on their relative orientations. The first and the second energy minima of Fig. 1(b) correspond to the two configurations of adjacent Walrafen pentamers with different mutual orientations (Fig. 1(c)).

The two local configurations—#1 and #2 in Fig. 1(c)—are (i) a high-energy, low specific volume, high-entropy, non-bonded #1-state, or (ii) a low-energy, high specific volume, low-entropy, bonded #2-state. The difference in local structure is also the difference in the local structure between a high-pressure crystalline ice (such as ice VI or ice VII) and a low-pressure crystalline ice (such as ice I_h) [34] (Fig. 1(c)).

The region of the P-T plane along the line continuing from the LDL-HDL coexistence line extrapolated to higher temperatures above the second critical point is the locus of points where the LDL on the low-pressure side and the HDL on the high-pressure side are continuously transforming—it is called the Widom line, defined to be the locus of points where the correlation length is maximum. Near this line, two different kinds of local structures, having either LDL or HDL properties, "coexist" [71, 126, 127]. The entropy fluctuations are largest near the Widom line, so C_P increases to a maximum, displaying a λ-like appearance [128]. The increase in C_P [58] resembles the signature of a glass transition as suggested by mode-coupling theory [129–131]. Careful measurements and simulations of static and dynamic

correlation functions [126,132–135] may be useful in determining the exact nature of the apparent singular behaviour near 220 K.

2.2 Potentials with two characteristic length scales: Tractable models

The above discussion is consistent with the possible existence of two well-defined classes of liquids: simple and water-like. The former interact via spherically-symmetric non-softened potentials, do not exhibit thermodynamic nor dynamic anomalies. We can calculate translational and orientational order parameters (t and q), and project equilibrium state points onto the (t, q) plane thereby generating what is termed the Errington-Debenedetti (ED) order map [43,136]. In water-like liquids, interactions are orientation-dependent; these liquids exhibit dynamic and thermodynamic anomalies, and their ED "order map" is in general two-dimensional but becomes linear (or quasi-linear) when the liquid exhibits structural, dynamic or thermodynamic anomalies.

Hemmer and Stell [137] showed that in fluids interacting via pairwise-additive, spherically-symmetric potentials consisting of a hard core plus an attractive tail, softening of the repulsive core can produce additional phase transitions. This pioneering study elicited a considerable body of work on so-called core-softened potentials which can generate water-like density and diffusion anomalies [137–147,151–156]. This important finding implies that strong orientational interactions, such as those that exist in water and silica, are not a necessary condition for a liquid to have thermodynamic and dynamic anomalies.

A softened-core potential has been used [122] to explain the isostructural solid-solid critical point present in materials such as Cs and Ce, for which the shape of the effective pair potential obtained from scattering experiments is "core-softened" [4,122,140,157,158]. Analytical work in 1D suggests a LL phase transition, and the existence at $T = 0$ of low and high density phases. Recent work using large-scale MD-simulations reports anomalous behaviour in 2D as well [140,142]. In 3D we showed that a squared potential with a repulsive shoulder and an attractive well displays a phase diagram with a LL critical point and no density anomaly [143–146]. The continuous version of the the same shouldered attractive potential shows not only the LL critical point, but also the density anomaly [147,156]. We use the soft-core potential to investigate the relationship between configurational entropy S_{conf} and diffusion coefficient D. Recent work using the SPC/E potential [159] suggests that the temperature-density dependence of S_{conf} may correlate with D, and that the maximum of S_{conf} tracks the density maxima line.

Two questions arise naturally from this emerging taxonomy of liquid behaviour. First, is structural order in core-softened fluids hard-sphere or water-like? Second, is it possible to seamlessly connect the range of liquid behaviour from hard spheres to water-like by a simple and common potential, simply by changing a physical parameter?

In recent work, Yan et al. [160–162] used a simple spherically-symmetric "hard-core plus ramp" potential to address the first question. They found that this core-softened potential with two characteristic length scales not only gives rise to water-like diffusive and density anomalies, but also to an ED water-like order map, implying that orientational interactions are not necessary in order for a liquid to have structural anomalies. We are investigating the evolution of dynamic, thermodynamic and structural anomalies, using the ratio λ of hard core and soft core length scales as a control parameter. We hope to show that the family of tunable spherically-symmetric potentials so generated evolves continuously between hard sphere and water-like behaviour; if successful, this will be the first demonstration that essential aspects of the wide range of liquid behaviour encompassed by hard spheres and tetrahedrally-coordinated network-formers can be systematically traversed by varying a single control parameter. We will study the equation of state, diffusion coefficient, and structural order parameters t and q. Our calculations seem to reveal a negative thermal expansion coefficient (static anomaly) and an increase of the diffusion coefficient upon isothermal compression (dynamic anomaly) for $0 \leq \lambda < 6/7$. As in bulk water, the regions where these anomalies occur are nested domes in the (T, ρ) or (T, P) planes, with the "thermodynamic anomaly dome" contained within the "dynamic anomaly dome." The ED order map evolves from water-like to hard-sphere-like upon varying between 4/7 and 6/7. Thus, we traverse the range of liquid behaviour encompassed by

hard spheres ($\lambda = 1$) and water-like ($\lambda \sim 4/7$) by simply varying the ratio of hard to soft-core diameters.

Further work is needed to establish whether a ratio of competing length scales close to 0.6 is generally associated with water-like anomalies in other core-softened potentials, e.g., achieving two characteristic length scales by using a linear combination of Gaussian [163] potentials of different widths.

In sum, motivated by the need to better understand the phenomenon of liquid polyamorphism [164–166], we are carrying out a systematic study of the effects of λ and the ratio of characteristic energies on the existence of a LL transition, the positive or negative slope of the line of first-order LL transitions in the (P,T) plane, and the relationship, if any [143,144], between the LL transition and density anomalies. We will perform calculations in parallel for both confined and bulk water.

3 Understanding "dynamic heterogeneities"

3.1 Recent experiments on confined water

Simulations and experiments both are consistent with the possibility that the LL critical point, if it exists at all, lies in the experimentally inaccessible No-Man's land. If this statement is valid, then at least two reactions are possible:

(i) If something is not experimentally accessible, then it does not deserve discussion.
(ii) If something is not experimentally accessible, but its influence *is* experimentally accessible, then discussion is warranted.

Option (ii) has guided most research thus far, since the manifestations of a critical point extend far away from the actual coordinates of that point. Indeed, accepting option (i) means there is nothing more to discuss. However if we confine water, the homogeneous nucleation temperature decreases and it becomes possible to enter the No-Man's land and, hence, search for the LL critical point. In fact, recent experiments at MIT and Messina by the Chen and Mallamace groups demonstrate that for nanopores of typically 1.5 nm diameter, the No-Man's land actually ceases to exist—one can supercool the liquid state all the way down to the glass temperature. Hence studying confined water offers the opportunity of directly testing, for the first time, the LL phase transition hypothesis.

In fact, using two independent techniques, neutron scattering and NMR, the MIT and Messina groups found a sharp kink in the dynamic properties (a "dynamic crossover") at the same temperature $T_L \approx 225\,\mathrm{K}$ [90,167]. Our calculations on *bulk* models [168] are not inconsistent with one tentative interpretation of this dynamic crossover as resulting from the system passing from the high-temperature high-pressure "HDL" side of the Widom line (where the liquid might display fragile behaviour) to the low-temperature low-pressure "LDL" side of the Widom line (where the liquid might display strong behaviour). By definition, the Widom line—defined to be the line in the pressure-temperature plane where the correlation length has its maximum—arises only if there is a critical point. Hence interpreting the MIT-Messina experiments in terms of a Widom line is of potential relevance to testing experimentally, for *confined* water, the liquid-liquid critical point hypothesis.

The interpretation of the dynamic crossover could have implications for nanofluidics and perhaps even for natural confined water systems, e.g., some proteins appear to undergo a change in their flexibility at approximately the same temperature T_L that the MIT-Messina experiments identify for the dynamic crossover in pure confined water.

3.2 Possible significance of the Widom line

The conjectured interpretation of the MIT-Messina experiments relies on the concept of the Widom line, a concept not widely appreciated even though it has been known by experimentalists dating back to the 1958 Ph.D. thesis of J.M.H. Levelt (now Levelt-Sengers) [171]. Since
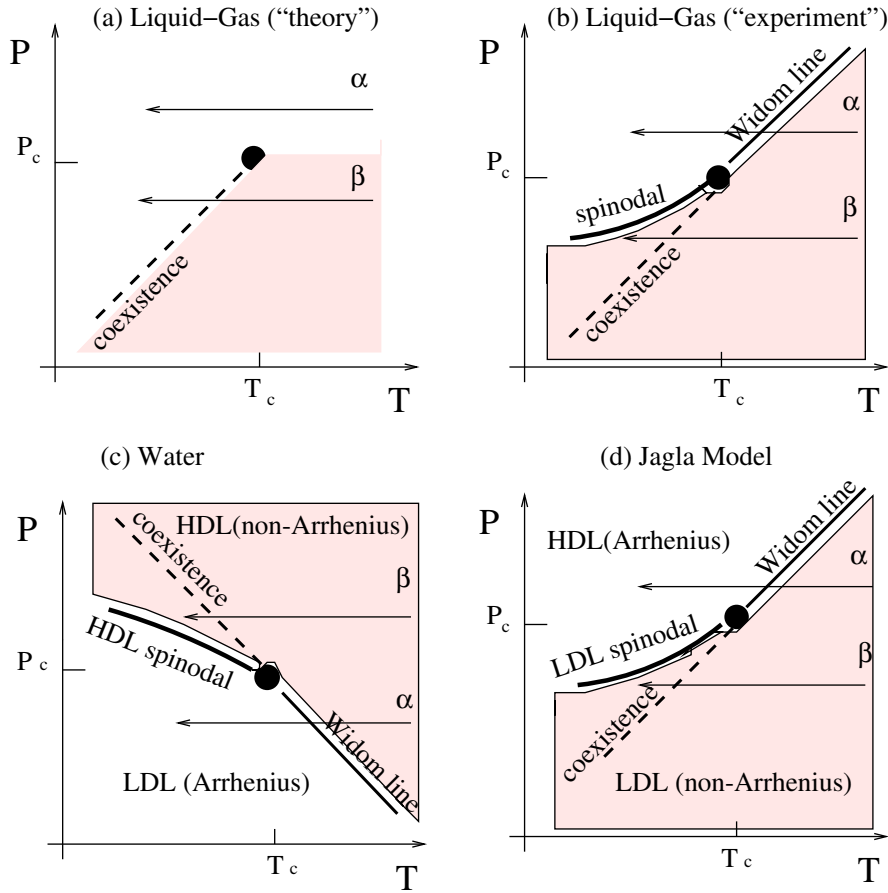
Fig. 2. (Colour online) (a) schematic phase diagram for the critical region associated with a liquid-gas critical point. Two features display mathematical singularities: the critical point and the liquid-gas coexistence. (b) Same, with the addition of the gas-liquid spinodal and the Widom line. Along the Widom line, thermodynamic response functions have extrema in their T dependence. (c) A hypothetical phase diagram for water of possible relevance to recent confined water neutron scattering experiments [90,167,169,170]. (d) A sketch of the $P-T$ phase diagram for the two-scale Jagla model.

a Widom line arises only from a critical point, if the MIT-Messina experiments can be rationalised by a Widom line then they are consistent with the existence of a LL critical point in confined water.

By definition, in a first order phase transition, thermodynamic functions discontinuously change as we cool the system along a path crossing the equilibrium coexistence line [Fig. 2(a), path β]. However in a *real* experiment, this discontinuous change may not occur at the coexistence line since a substance can remain in a supercooled metastable phase until a limit of stability (a spinodal) is reached [4] [Fig. 2(b), path β].

If the system is cooled isobarically along a path above the critical pressure P_c [Fig. 2(b), path α], the state functions continuously change from the values characteristic of a high temperature phase (gas) to those characteristic of a low temperature phase (liquid). The thermodynamic response functions which are the derivatives of the state functions with respect to temperature [e.g., C_P] have maxima at temperatures denoted $T_{\max}(P)$. Remarkably these maxima are still prominent far above the critical pressure [171,172], and the values of the response functions at $T_{\max}(P)$ (e.g., $C_P^{\max}$) diverge as the critical point is approached. The lines of the maxima for different response functions asymptotically approach one another as the critical point is approached, since all response functions become expressible in terms of the correlation length.

This asymptotic line is sometimes called the Widom line, and is often regarded as an extension of the coexistence line into the "one-phase regime."

Suppose now that the system is cooled at constant pressure P_0. (i) If $P_0 > P_C$ ("path α"), experimentally-measured quantities will change dramatically but continuously in the vicinity of the Widom line (with huge fluctuations as measured by, e.g., C_P). (ii) If $P_0 < P_C$ ("path β"), experimentally-measured quantities will change discontinuously if the coexistence line is actually seen. However the coexistence line can be difficult to detect in a pure system due to metastability, and changes will occur only when the spinodal is approached where the gas phase is no longer stable.

In the case of water—the most important solvent for biological function [173, 174]—a significant change in dynamical properties has been suggested to take place in deeply supercooled states [175–178]. Unlike other network forming materials [179], water behaves as a fragile liquid in the experimentally accessible window [176, 180, 181]. Based on analogies with other network forming liquids and with the thermodynamic properties of the amorphous forms of water, it has been suggested that, at ambient pressure, liquid water should show a crossover between fragile behaviour at high T to strong behaviour at low T [138, 139, 177, 182, 183] in the deep supercooled region of the phase diagram below the homogeneous nucleation line. This region may contain the hypothesised LL critical point [44], the terminal point of a line of first order LL phase transitions. Recently, dynamic crossovers in confined water were studied experimentally [90, 96, 169, 184] since nucleation can be avoided in confined geometries. Also, a dynamic crossover has been associated with the LL phase transition in both silicon and silica [185, 186]. In the following, we offer a very tentative interpretation of the observed fragility transition in water as arising from crossing the Widom line emanating from the hypothesised LL critical point [186] [Fig. 2, path α].

3.3 Methods employed to study dynamic crossovers in confined water

Using MD-simulations [187], we study three models, each of which has a LL critical point. Two of the models, (the TIP5P [68] and the ST2 [188]) treat water as a multiple site rigid body, interacting via electrostatic site-site interactions complemented by a Lennard-Jones potential. The third model is the spherically symmetric "two-scale" Jagla potential with attractive and repulsive ramps which has been recently studied in the context of LL phase transitions and liquid anomalies [157, 151]. For all three models, we evaluate the loci of maxima of the relevant response functions, K_T and C_P, which coincide close to the critical point and give rise to the Widom line. We carefully explore the hypothesis that, for all three potentials, a dynamic crossover occurs when the Widom line is crossed.

For TIP5P we find a LL critical point [69, 70], from which the Widom line develops. The coexistence curve is negatively sloped, so the Clapeyron equation implies that the high-temperature phase is a high-density liquid (HDL) and the low-temperature phase is a low-density liquid (LDL). The diffusion coefficient D is evaluated from the long time limit of the mean square displacement along isobars. We find that isobars crossing the Widom line (path α) show a clear crossover (i) from a *non-Arrhenius behaviour at high T* [which can be well fitted by a power law function $D \sim (T - T_{\mathrm{MCT}})^{\gamma}$], consistent with the mode coupling theory predictions [189]), (ii) to an *Arrhenius behaviour at low T* [which can be described by $D \sim \exp(-E_a/T)$]. The crossover between these two functional forms takes place when crossing the Widom line.

For paths β, crystallisation occurs in TIP5P [69], so the hypothesis that there is no fragility transition cannot be checked at low temperature. Hence we consider a related potential, ST2, for which crystallisation is absent within the time scale of the simulation. Simulation details are described in [190]. This potential also displays a LL critical point [44, 190]. Along paths α a fragility transition may take place, while along paths β the T dependence of D does not show any sign of crossover to Arrhenius behaviour and the fragile behaviour is retained down to the lowest studied temperature. Indeed, for paths β, the entire T dependence can be fit by a power law $(T - T_{\mathrm{MCT}})^{\gamma}$.

If indeed TIP5P and ST2 water models support the connection between the Widom line and the dynamic fragility transition, it is natural to ask which features of the water molecular

potential are responsible for the properties of water, especially because water's unusual properties are shared by several other liquids whose inter-molecular potential has two energy (length) scales such as silicon and silica [185, 186, 191]. Hence we also investigate the two-scale spherically symmetric Jagla potential [138, 139, 157], displaying – without the need to supercool – a LL coexistence line which, unlike water, has a positive slope, implying that the Widom line is now crossed along α paths with $P > P_C$. We verify a crossover in the behaviour of $D(T)$ when the Widom line ($C_P^{\max}$ line) is crossed, such that at high temperature, D exhibits an Arrhenius behaviour, while at low temperature it follows a non-Arrhenius behaviour, consistent with a power law. Along a β path ($P < P_C$), $D(T)$ appears to follow the Arrhenius behaviour over the entire studied temperature range. Thus we test that the dynamic crossover coincides with the location of the $C_P^{\max}$ line, extending the conclusion of the TIP5P and ST2 potentials to a general two-scale spherically symmetric potential.

4 Hamiltonian model of water

In Ref. [148], we investigated the generality of the dynamic crossover in a Hamiltonian model of water which displays a liquid-liquid phase transition at low temperatures. We consider a cell model that reproduces the fluid phase diagram of water and other tetrahedral network forming liquids [50–53]. For sake of clarity, we focus on water to explain the motivation of the model. The model is based on the experimental observations that on decreasing P at constant T, or on decreasing T at constant P, (i) water displays an increasing local tetrahedrality [149], (ii) the volume per molecule increases at sufficiently low P or T, and (iii) the O-O-O angular correlation increases [74], consistent with simulations [150].

The system is divided into cells $i \in [1, \ldots, N]$ on a regular square lattice, each containing a molecule with volume $v \equiv V/N$, where $V \geq Nv_0$ is the total volume of the system, and v_0 is the hard-core volume of one molecule. The cell volume v is a continuous variable that gives the mean distance $r \equiv v^{1/d}$ between molecules in d dimensions. The van der Waals attraction between the molecules is represented by a truncated Lennard-Jones potential with characteristic energy $\epsilon > 0$

$$U(r) \equiv \begin{cases} \infty & \text{for } r \leq R_0 \\ \epsilon \left[\left(\dfrac{R_0}{r} \right)^{12} - \left(\dfrac{R_0}{r} \right)^6 \right] & \text{for } r > R_0, \end{cases} \tag{1}$$

where $R_0 \equiv v_0^{1/d}$ is the hard-core distance [148].

Each molecule i has four bond indices $\sigma_{ij} \in [1, \ldots, q]$, corresponding to the nearest-neighbour cells j. When two nearest-neighbour molecules have the facing σ_{ij} and σ_{ji} in the same relative orientation, they decrease the energy by a constant J, with $0 < J < \epsilon$, and form a bond, e.g. a (non-bifurcated) hydrogen bond for water, or a ionic bond for SiO$_2$. The choice $J < \epsilon$ guarantees that bonds are formed only in the liquid phase. Bonding and intramolecular (IM) interactions are accounted for by the two Hamiltonian terms

$$\mathcal{H}_{\mathrm{B}} \equiv -J \sum_{\langle i,j \rangle} \delta_{\sigma_{ij}\sigma_{ji}}, \tag{2}$$

where the sum is over n.n. cells, $0 < J < \epsilon$ is the bond energy, $\delta_{a,b} = 1$ if $a = b$ and $\delta_{a,b} = 0$ otherwise, and

$$\mathcal{H}_{\mathrm{IM}} \equiv -J_\sigma \sum_i \sum_{(k,\ell)_i} \delta_{\sigma_{ik}\sigma_{i\ell}}, \tag{3}$$

where $\sum_{(k,\ell)_i}$ denotes the sum over the IM bond indices (k, l) of the molecule i and $J_\sigma > 0$ is the IM interaction energy with $J_\sigma < J$, which models the angular correlation between the bonds on the same molecule. The total energy of the system is the sum of the van der Waals interaction and Eqs. (2) and (3).
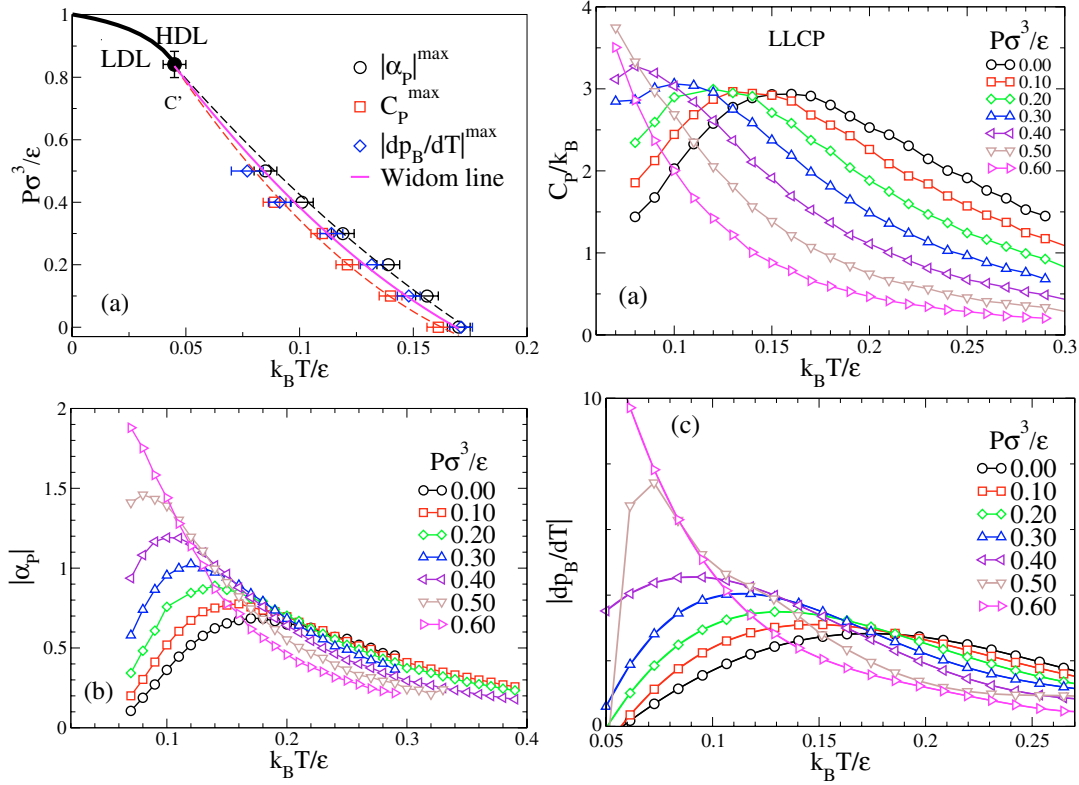
Fig. 3. (Colour online) (a) phase diagram below T_{MD} line shows that $|dp_{\mathrm{B}}/dT|^{\mathrm{max}}$ ($\diamond$) coincides with the Widom line $T_W(P)$ (solid line) within error bars: C' is the HDL-LDL critical point, end of first-order phase transition line (thick line) [148]; symbols are maxima for $N = 3600$ of $|\alpha_P|^{\mathrm{max}}$ ($\circ$), C_P^{max} ($\square$), and $|dp_{\mathrm{B}}/dT|^{\mathrm{max}}$ ($\diamond$); upper and lower dashed line are quadratic fits of $|\alpha_P|^{\mathrm{max}}$ and C_P^{max}, respectively, consistent with C'; $|\alpha_P|^{\mathrm{max}}$ and C_P^{max} are consistent within error bars. Maxima are estimated from panels (b), (c) and (d), where each quantity is shown as functions of T for different $P < P_{C'}$. In (e) $|dp_{\mathrm{B}}/dT|^{\mathrm{max}}$ is the numerical derivative of p_{B} from simulations in (d).

We find that different response functions such as C_P, α_p (see Fig. 3) show maxima and these maxima increase and seem to diverge as the critical pressure is approached, consistent with the picture of Widom line that we discussed for other water models in the sections above. Moreover we find that the temperature derivative of the number of hydrogen bonds dN_{HB}/dT displays a maximum in the same region where the other thermodynamic response functions have maxima; suggesting that the fluctuations in the number of hydrogen bonds is maximum at the Widom line temperature T_W.

To futher test if this model system also displays a dynamic crossover as found in the other models of water, we study the total spin relaxation time of the system as a function of T for different pressures. We find that for $J_\sigma/\epsilon = 0.05$ (*liquid-liquid critical point scenario*) the crossover occurs at $T_W(P)$ for $P < P_{C'}$ [Fig. 4(a)]. For completeness we study the system also in the case of *singularity free scenario*, corresponding to $J_\sigma = 0$. For $J_\sigma = 0$ the crossover is at $T(C_P^{\mathrm{max}})$, the temperature of C_P^{max} [Fig. 4(b)].

We next calculate the Arrhenius activation energy $E_{\mathrm{A}}(P)$ from the low-T slope of $\log \tau$ vs. $1/T$ [Fig. 5(a)]. We extrapolate the temperature $T_{\mathrm{A}}(P)$ at which τ reaches a fixed macroscopic time $\tau_{\mathrm{A}} \geq \tau_{\mathrm{C}}$. We choose $\tau_{\mathrm{A}} = 10^{14}$ MC steps > 100 sec [131] [Fig. 5(b)]. We find that $E_{\mathrm{A}}(P)$ and $T_{\mathrm{A}}(P)$ decrease upon increasing P in both scenarios, providing no distinction between the two interpretations. Instead, we find a dramatic difference in the P dependence of the quantity $E_{\mathrm{A}}/(k_B T_{\mathrm{A}})$ in the two scenarios, increasing for the LL critical point scenario and approximately constant for the singularity free scenario [Fig. 5(c)].
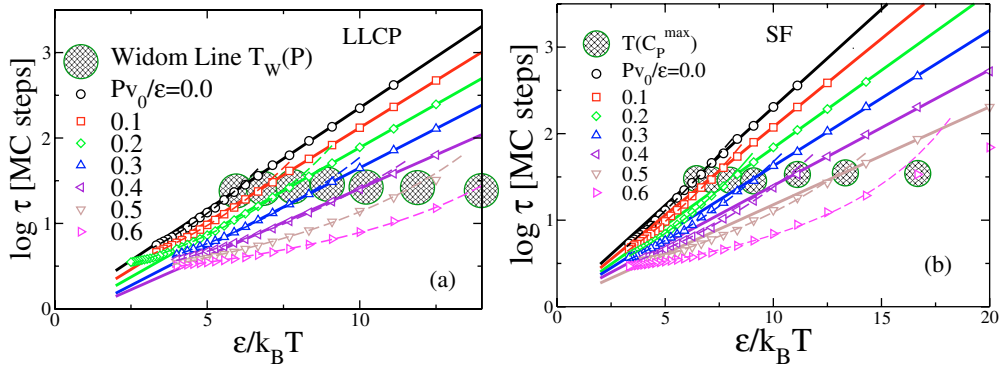
Fig. 4. (Colour online) dynamic crossover—large hatched circles of a radius approximately equal to the error bar—in the orientational relaxation time τ for a range of different pressures. (a) The LL critical point (LLCP) scenario, with crossover temperature at $T_W(P)$. (b) The singularity free (SF) scenario, with crossover temperature at $T(C_P^{\max})$. Solid and dashed lines represent Arrhenius and non-Arrhenius fits, respectively. Notice that the dynamic crossover occurs at approximately the same value of τ for all seven values of pressure studied.
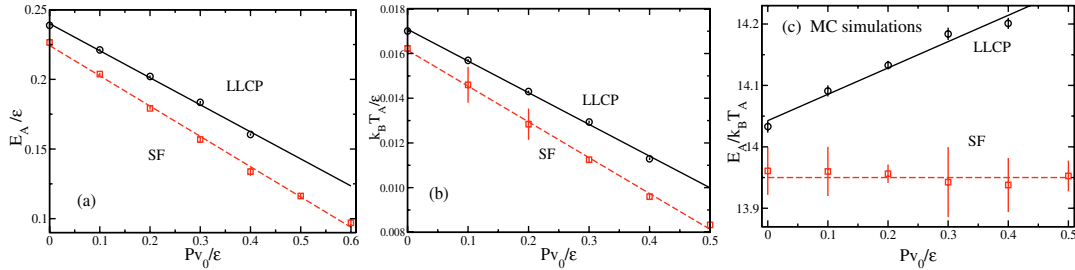
Fig. 5. (Colour online) effect of pressure on the activation energy E_A. (a) Demonstration that E_A decreases linearly for increasing P for both the LL critical point and the singularity free scenarios. The lines are linear fits to the simulation results (symbols). (b) T_A, defined such that $\tau(T_A) = 10^{14}$ MC steps > 100 sec [131], decreases linearly with P for both scenarios. (c) P dependence of the quantity $E_A/(k_B T_A)$ is different in the two scenarios. In the LL critical point (LLCP) scenario, $E_A/(k_B T_A)$ increases with increasing P, and it is approximately constant in the singularity free (SF) scenario. The lines are guides to the eyes.

5 Outlook

It is possible that other phenomena that appear to occur on crossing the Widom line are in fact not coincidences, but are related to the changes in local structure that occur when the system changes from the "HDL-like" side to the "LDL-like" side. In this work we concentrated on reviewing the evidence for changes in dynamic transport properties, such as diffusion constant and relaxation time. Additional examples include: (1) a breakdown of the Stokes-Einstein relation for $T < T_W(P)$ [192–197], (2) systematic changes in the static structure factor $S(q)$ and the corresponding pair correlation function $g(r)$ revealing that for $T < T_W(P)$ the system more resembles the structure of LDL than HDL, (3) appearance for $T < T_W(P)$ of a shoulder in the dynamic structure factor $S(q,\omega)$ at a frequency $\omega \approx 60\,\mathrm{cm}^{-1} \approx 2\,\mathrm{THz}$ [198,199], (4) rapid increase in hydrogen bonding degree for $T < T_W(P)$ [200,201], (5) a *minimum* in the density at low temperature [202], and (6) a scaled equation of state near the critical point [203]. It is important to know how general a given phenomenon is, such as crossing the Widom line which by definition is present whenever there is a critical point. Using data on other liquids which have local tetrahedral symmetry, such as silicon and silica, which appear to also display a liquid-liquid critical point and hence must possess a Widom line emanating from this point into the one-phase region. For example, we learned of interesting new work on silicon, which

also interprets structural changes as arising from crossing the Widom line of silicon [204]. It might be interesting to test the effect of the Widom line on simple model systems that display a liquid-liquid critical point, such as two-scale symmetric potentials of the sort recently studied by Xu and her collaborators [205] or by Franzese [147] and Barros de Oliveira and coworkers [156].

Very recently, Mallamace and his collaborators succeeded in locating the Widom line by finding a clearcut maximum in the coefficient of thermal expansion, at $T_W \approx 225\,\mathrm{K}$ [206–208], which remarkably is the same temperature as the specific heat maximum [209]. Also, private discussions with Jacob Klein reveal a possible reason for why confined water does not freeze at $-38\,°\mathrm{C}$, the bulk homogeneous nucleation temperature: Klein and co-workers [210] noted that confined water behaves differently than typical liquids in that it water does not experience the huge increase in viscosity characteristic of other strongly confined liquids. They interpret this experimental finding as arising from the fact that strong confinement hampers the formation of a hydrogen bonded network, and we know from classic work of Linus Pauling that without the extensive hydrogen bonded network, water's freezing temperature will be depressed by more than 100 degrees. Thus confinement reduces the extent of the hydrogen bonded network and hence lowers the freezing temperature, but leaves the key tetrahedral local geometry of the water molecule itself unchanged.

Note added in proof: After this work has been submitted, it was demonstrated that the solubility of hard spheres and hard-spheres "bead-on-a-string polymers" in the two-scale spherically-symmetric Jagla ramp potential dramatically changes upon crossing the Widom line with the HDL-like phase being a poorer solvent than the LDL-like phase [211]. A similar effect was observed in simulations of hydrophobic particles in TIP5P water [70].

References

1. R. Waller, trans., *Essayes of Natural Experiments* [original in Italian by the Secretary of the Academie del Cimento], Facsimile of 1684 English translation (Johnson Reprint Corporation, New York, 1964)
2. H.E. Stanley, Mat. Res. Bull. **24**, 22 (1999)
3. C.A. Angell, M. Oguni, W.J. Sichina, J. Phys. Chem. **86**, 998 (1982)
4. P.G. Debenedetti, H.E. Stanley, Physics Today **56**, 40 (2003)
5. O. Mishima, H.E. Stanley, Nature **396**, 329 (1998)
6. R.J. Speedy, C.A. Angell, J. Chem. Phys. **65**, 851 (1976)
7. E.F. Burton, W.F. Oliver, Proc. Roy. Soc. London Ser. A **153**, 166 (1936)
8. O. Mishima, L.D. Calvert, E. Whalley, Nature **310**, 393 (1984)
9. H.-G. Heide, Ultramicroscopy **14**, 271 (1984)
10. O. Mishima, L.D. Calvert, E. Whalley, Nature **314**, 76 (1985)
11. M.C. Bellissent-Funel, L. Bosio, A. Hallbrucker, E. Mayer, R. Sridi-Dorbez, J. Chem. Phys. **97**, 1282 (1992)
12. M.C. Bellissent-Funel, L. Bosio, J. Chem. Phys. **102**, 3727 (1995)
13. K.H. Smith, E. Shero, A. Chizmeshya, G.H. Wolf, J. Chem. Phys. **102**, 6851 (1995)
14. P.H. Poole, T. Grande, F. Sciortino, H.E. Stanley, C.A. Angell, J. Comp. Mat. Sci. **4**, 373 (1995)
15. J.L. Finney, Phil. Trans. R. Soc. Lond. B: Biol. Sci. **359**, 1145 (2004)
16. E. Mayer, in *Hydrogen Bond Networks*, edited by M.-C. Bellissent-Funel, J.C. Dore (Kluwer Academic Publishers, Dordrecht, 1994), p. 355
17. O. Mishima, Nature **384**, 546 (1996)
18. G.P. Johari, A. Hallbrucker, E. Mayer, Science **273**, 90 (1996)
19. U. Essmann, A. Geiger, J. Chem. Phys. **103**, 4678 (1995)
20. T. Loerting, C. Salzmann, I. Kohl, E. Mayer, A. Hallbrucker, Phys. Chem. Chem. Phys. **3**, 5355 (2001)
21. J.L. Finney, D.T. Bowron, A.K. Soper, T. Loerting, E. Mayer, A. Hallbrucker, Phys. Rev. Lett. **89**, 503 (2002)

22. J.S. Tse, D.D. Klug, M. Guthrie, C.A. Tulk, C.J. Benmore, J. Urquidi, Phys. Rev. B **71**, 214107 (2005)
23. I. Brovchenko, A. Geiger, A. Oleinikova, J. Chem. Phys. **118**, 9473 (2003)
24. I. Brovchenko, A. Geiger, A. Oleinikova, J. Chem. Phys. **123**, 044515 (2005)
25. P. Jedlovszky, R. Vallauri, J. Chem. Phys. **122**, 081101 (2005)
26. J.A. White, Physica A **346**, 347 (2004)
27. J.K. Christie, M. Guthrie, C.A. Tulk, C.J. Benmore, D.D. Klug, S.N. Taraskin, S.R. Eliot, Phys. Rev. B **72**, 012201 (2005)
28. J.L. Finney, A. Hallbrucker, I. Kohl, A.K. Soper, D.T. Bowron, Phys. Rev. Lett. **88**, 225503 (2002)
29. D. Eisenberg, W. Kauzmann, *The Structure and Properties of Water* (Oxford University Press, New York, 1969)
30. J.D. Bernal, R.H. Fowler, J. Chem. Phys. **1**, 515 (1933)
31. J.A. Pople, Proc. Roy. Soc. Lond. Ser. A **205**, 163 (1951)
32. H.S. Frank, W.-Y. Wen, Disc. Faraday Soc. **24**, 133 (1957)
33. G. Némethy, H.A. Scheraga, J. Chem. Phys. **36**, 3382 (1962)
34. B. Kamb, in *Structural Chemistry and Molecular Biology*, edited by A. Rich, N. Davidson (Freeman, San Francisco, 1968), p. 507
35. W.C. Röntgen, Ann. d. Phys. u. Chem. **45**, 91 (1892)
36. L. Pauling, in *Hydrogen Bonding*, edited by D. Hadzi (Pergamon Press, New York, 1959), p. 1
37. R.J. Speedy, J. Phys. Chem. **86**, 982 (1982)
38. S. Sastry, P. Debenedetti, F. Sciortino, H.E. Stanley, Phys. Rev. E **53**, 6144 (1996)
39. H.E. Stanley, J. Teixeira, A. Geiger, R.L. Blumberg, Physica A **106**, 260 (1981)
40. H.E. Stanley, J. Phys. A **12**, L329 (1979)
41. H.E. Stanley, J. Teixeira, J. Chem. Phys. **73**, 3404 (1980)
42. A. Geiger, H.E. Stanley, Phys. Rev. Lett. **49**, 1749 (1982)
43. J.R. Errington, P.G. Debenedetti, S. Torquato, Phys. Rev. Lett. **89**, 215503 (2002)
44. P.H. Poole, F. Sciortino, U. Essmann, H.E. Stanley, Nature **360**, 324 (1992)
45. E.G. Ponyatovskii, V.V. Sinitsyn, T.A. Pozdnyakova, JETP Lett. **60**, 360 (1994)
46. C.T. Moynihan, Mat. Res. Soc. Symp. Proc. **455**, 411 (1997)
47. P.H. Poole, F. Sciortino, T. Grande, H.E. Stanley, C.A. Angell, Phys. Rev. Lett. **73**, 1632 (1994)
48. S.S. Borick, P.G. Debenedetti, S. Sastry, J. Phys. Chem. **99**, 3781 (1995)
49. C.F. Tejero, M. Baus, Phys. Rev. E **57**, 4821 (1998)
50. G. Franzese, H.E. Stanley, Physica A **314**, 508 (2002)
51. G. Franzese, H.E. Stanley, J. Phys.: Cond. Mat. **14**, 2193 (2002)
52. G. Franzese, M.I. Marqués, H.E. Stanley, Phys. Rev. E. **67**, 011103 (2003)
53. G. Franzese, H.E. Stanley, J. Phys.: Cond. Mat. **19**, 205126 (2007)
54. H. Kanno, R. Speedy, C.A. Angell, Science **189**, 880 (1975)
55. O. Mishima, J. Chem. Phys. **100**, 5910 (1994)
56. O. Mishima, H.E. Stanley, Nature **392**, 164 (1998)
57. E. Whalley, D.D. Klug, Y.P. Handa, Nature **342**, 782 (1989)
58. G.P. Johari, G. Fleissner, A. Hallbrucker, E. Mayer, J. Phys. Chem. **98**, 4719 (1994)
59. R.J. Speedy, P.G. Debenedetti, R.S. Smith, C. Huang, B.D. Kay, J. Chem. Phys. **105**, 240 (1996)
60. L.S. Bartell, J. Huang, J. Phys. Chem. **98**, 7455 (1994)
61. P. Brüggeller, E. Mayer, Nature **288**, 569 (1980)
62. P.W. Bridgman, J. Chem. Phys. **3**, 597 (1935)
63. P.H. Poole, U. Essmann, F. Sciortino, H.E. Stanley, Phys. Rev. E **48**, 4605 (1993)
64. H. Tanaka, J. Chem. Phys. **105**, 5099 (1996)
65. S. Harrington, R. Zhang, P.H. Poole, F. Sciortino, H.E. Stanley, Phys. Rev. Lett. **78**, 2409 (1997)
66. F. Sciortino, P.H. Poole, U. Essmann, H.E. Stanley, Phys. Rev. E **55**, 727 (1997)
67. S. Harrington, P.H. Poole, F. Sciortino, H.E. Stanley, J. Chem. Phys. **107**, 7443 (1997)
68. W.L. Jorgensen, J. Chandrasekhar, J. Madura, R.W. Impey, M. Klein, J. Chem. Phys. **79**, 926 (1983)
69. M. Yamada, S. Mossa, H.E. Stanley, F. Sciortino, Phys. Rev. Lett. **88**, 195701 (2002)
70. D. Paschek, Phys. Rev. Lett. **94**, 217802 (2005)
71. E. Shiratani, M. Sasai, J. Chem. Phys. **108**, 3264 (1998)
72. M.-C. Bellissent-Funel, Europhys. Lett. **42**, 161 (1998)
73. H.E. Stanley, S.V. Buldyrev, M. Canpolat, O. Mishima, M.R. Sadr-Lahijany, A. Scala, F.W. Starr, Phys. Chem. Chem. Phys. **2**, 1551 (2000)

74. A.K. Soper, M.A. Ricci, Phys. Rev. Lett. **84**, 2881 (2000) and references therein
75. A.C. Mitus, A.Z. Patashinskii, B.I. Shumilo, Phys. Lett. A **113**, 41 (1985)
76. A.C. Mitus, A.Z. Patashinskii, Acta Phys. Pol. A **74**, 779 (1988)
77. R. Zangi, A.E. Mark, J. Chem. Phys. **119**, 1694 (2003)
78. R. Zangi, J. Phys.: Cond. Mat. **16**, S5371 (2004)
79. P.M. Wiggins, Microbio. Rev. **54**, 432 (1990)
80. P.M. Wiggins, Prog. Polym. Sci. **20**, 1121 (1995)
81. M.-C. Bellissent-Funel, J.-M. Zanotti, S.H. Chen, Faraday Discuss. **103**, 281 (1996)
82. V. Crupi, S. Magazu, D. Majolino, P. Migliardo, V. Venuti, M.-C. Bellissent-Funel, J. Phys.: Cond. Mat. **12**, 3625 (2000)
83. M.-C. Bellissent-Funel, J. Mol. Liq. **84**, 39 (2000)
84. M.-C. Bellissent-Funel, S.H. Chen, J.M. Zanotti, Phys. Rev. E **51**, 4558 (1995)
85. M.-C. Bellissent-Funel, J. Teixeira, K.F. Bradley, S.H. Chen, J. Phys. I (France) **2**, 995 (1992)
86. S.H. Chen, P. Gallo, M.-C. Bellissent-Funel, Canadian J. Phys. **73**, 703 (1995)
87. Z. Dohnálek, G.A. Kimmel, R.L. Ciolli, K.P. Stevenson, R.S. Smith, B.D. Kay, J. Chem. Phys. **112**, 5932 (2000)
88. T.M. Truskett, P.G. Debenedetti, S. Torquato, J. Chem. Phys. **114**, 2401 (2001)
89. J.-M. Zanotti, M.-C. Bellissent-Funel, S.-H. Chen, Europhys. Lett. **71**, 91 (2005)
90. L. Liu, S.-H. Chen, A. Faraone, C.-W. Yen, C.Y. Mou, Phys. Rev. Lett. **95**, 117802 (2005)
91. M.E. Green, J. Lu, J. Coll. Int. Sci. **171**, 117 (1995)
92. K. Koga, X.C. Zeng, H. Tanaka, Phys. Rev. Lett. **79**, 5262 (1997)
93. J. Slovak, K. Koga, H. Tanaka, X.C. Zeng, Phys. Rev. E **60**, 5833 (1999)
94. K. Koga, X.C. Zeng, H. Tanaka, Chem. Phys. Lett. **285**, 278 (1998)
95. K. Koga, H. Tanaka, X.C. Zeng, Nature **408**, 564 (2000)
96. R. Bergman, J. Swenson, Nature **403**, 283 (2000)
97. J. Teixeira, J.M. Zanotti, M.-C. Bellissent-Funel, S.H. Chen, Physica B **234**, 370 (1997)
98. P. Gallo, Phys. Chem. Phys. **2**, 1607 (2000)
99. P. Gallo, M. Rovere, M.A. Ricci, C. Hartnig, E. Spohr, Europhys. Lett. **49**, 183 (2000)
100. P. Gallo, M. Rovere, M.A. Ricci, C. Hartnig, E. Spohr, Phil. Mag. B **79**, 1923 (1999)
101. M. Rovere, M.A. Ricci, D. Vellati, F. Bruni, J. Chem. Phys. **108**, 9859 (1998)
102. M.-C. Bellissent-Funel, R. Sridi-Dorbez, L. Bosio, J. Chem. Phys. **104**, 10023 (1996)
103. J. Forsman, B. Jonsson, C.E. Woodward, J. Phys. Chem. **100**, 15005 (1996)
104. M. Meyer, H.E. Stanley, J. Phys. Chem. B **103**, 9728 (1999)
105. P.A. Netz, T. Dorfmuller, J. Phys. Chem. B **102**, 4875 (1998)
106. J.-M. Zanotti, M.-C. Bellissent-Funel, S.H. Chen, Phys. Rev. E **59**, 3084 (1999)
107. M.-C. Bellissent-Funel, J. Teixeira, in *Freeze-drying/Lyophilization of Pharmaceutical and Biological Products*, edited by L. Rey, J.C. May (Marcel Dekker, New York, 1999), Chap. 3, p. 53
108. H. Tanaka, I. Ohmine, J. Chem. Phys. **87**, 6128 (1987)
109. I. Ohmine, H. Tanaka, P.G. Wolynes, J. Chem. Phys. **89**, 5852 (1988)
110. H. Tanaka, I. Ohmine, J. Chem. Phys. **91**, 6318 (1989)
111. I. Ohmine, H. Tanaka, J. Chem. Phys. **93**, 8138 (1990)
112. I. Ohmine, H. Tanaka, in *Molecular Dynamics Simulations*, edited by F. Yonezawa (Springer Verlag, Berlin, 1991), p. 130
113. I. Okabe, H. Tanaka, K. Nakanishi, Phys. Rev. E **53**, 2638 (1996)
114. H. Tanaka, in *ACS Symposium Series on Experimental and Theoretical Approaches to Supercooled Liquids*, edited by J. Fourkas (ACS, 1997), Chap. 18, p. 233
115. T. Kabeya, Y. Tamai, H. Tanaka, J. Phys. Chem. B **102**, 899 (1998)
116. Y. Tamai, H. Tanaka, Phys. Rev. E **59**, 5647 (1999)
117. H. Tanaka, R. Yamamoto, K. Koga, X.C. Zeng, Chem. Phys. Lett. **304**, 378 (1999)
118. J. Slovak, K. Koga, H. Tanaka, X.C. Zeng, Phys. Rev. E **60**, 5833 (1999)
119. G.T. Gao, X.C. Zeng, H. Tanaka, J. Chem. Phys. **112**, 8534 (2000)
120. M.-C. Bellissent-Funel, Eur. Phys. J. E **12**, 83 (2003)
121. M.-C. Bellissent-Funel, C. R. Geoscience **337**, 173 (2005)
122. P.C. Hemmer, G. Stell, Phys. Rev. Lett. **24**, 1284 (1970)
123. M. Canpolat, F.W. Starr, M.R. Sadr-Lahijany, A. Scala, O. Mishima, S. Havlin, H.E. Stanley, Chem. Phys. Lett. **294**, 9 (1998)
124. S. Sastry, F. Sciortino, H.E. Stanley, J. Chem. Phys. **98**, 9863 (1993)
125. C.J. Roberts, A.Z. Panagiotopulos, P.G. Debenedetti, Phys. Rev. Lett. **77**, 4386 (1996)

126. E. Shiratani, M. Sasai, J. Chem. Phys. **104**, 7671 (1996)
127. H. Tanaka, Phys. Rev. Lett. **80**, 113 (1998)
128. C.A. Angell, J. Shuppert, J.C. Tucker, J. Phys. Chem. **77**, 3092 (1973)
129. F. Sciortino, L. Fabbian, S.-H. Chen, P. Tartaglia, Phys. Rev. E **56**, 5397 (1997)
130. F. Sciortino, P. Gallo, P. Tartaglia, S.-H. Chen, Phys. Rev. E **54**, 6331 (1996)
131. P. Kumar, G. Franzese, S.V. Buldyrev, H.E. Stanley, Phys. Rev. E **73**, 041505 (2006)
132. Y. Xie, K.F. Ludwig, G. Morales, D.E. Hare, C.M. Sorensen, Phys. Rev. Lett. **71**, 2051 (1993)
133. F. Sciortino, P. Poole, H.E. Stanley, S. Havlin, Phys. Rev. Lett. **64**, 1686 (1990)
134. A. Luzar, D. Chandler, Nature **379**, 55 (1996); A. Luzar, D. Chandler, Phys. Rev. Lett. **76**, 928 (1996)
135. F.W. Starr, J.K. Nielsen, H.E. Stanley, Phys. Rev. Lett. **82**, 2294 (1999); F.W. Starr, J.K. Nielsen, H.E. Stanley, Phys. Rev. E **62**, 579 (2000)
136. J.R. Errington, P.G. Debenedetti, Nature **409**, 318 (2001)
137. J.M. Kincaid, G. Stell, C.K. Hall, J. Chem. Phys. **65**, 2161 (1976)
138. E.A. Jagla, J. Phys. Cond. Mat. **11**, 10251 (1999)
139. E.A. Jagla, Phys. Rev. E **63**, 061509 (2001)
140. M.R. Sadr-Lahijany, A. Scala, S.V. Buldyrev, H.E. Stanley, Phys. Rev. Lett. **81**, 4895 (1998)
141. A. Scala, M.R. Sadr-Lahijany, N. Giovambattista, S.V. Buldyrev, H.E. Stanley, Phys. Rev. E **63**, 041202 (2001)
142. A. Scala, M.R. Sadr-Lahijany, N. Giovambattista, S.V. Buldyrev, H.E. Stanley, J. Stat. Phys. **100**, 97 (2000)
143. G. Franzese, G. Malescio, A. Skibinsky, S.V. Buldyrev, H.E. Stanley, Nature **409**, 692 (2001)
144. G. Franzese, G. Malescio, A. Skibinsky, S.V. Buldyrev, H.E. Stanley, Phys. Rev. E **66**, 051206 (2002)
145. A. Skibinsky, S.V. Buldyrev, G. Franzese, G. Malescio, H.E. Stanley, Phys. Rev. E **69**, 061206 (2004)
146. G. Malescio, G. Franzese, A. Skibinsky, S.V. Buldyrev, H.E. Stanley, Phys. Rev. E **71**, 061504 (2005)
147. G. Franzese, J. Mol. Liq. **136**, 267 (2007)
148. P. Kumar, G. Franzese, H.E. Stanley, Phys. Rev. Lett. **100**, 105701 (2008)
149. G. D'Arrigo, G. Maisano, F. Mallamace, P. Migliardo, S. Wanderlingh, J. Chem. Phys. **75**, 4264 (1981); C.A. Angell, V. Rodgers, J. Chem. Phys. **80**, 6245 (1984)
150. E. Schwegler, G. Galli, F. Gygi, Phys. Rev. Lett. **84**, 2429 (2000); P. Raiteri, A. Laio, M. Parrinello, Phys. Rev. Lett. **93**, 087801 (2004) and references cited therein
151. P. Kumar, S.V. Buldyrev, F. Sciortino, E. Zaccarelli, H.E. Stanley, Phys. Rev. E **72**, 021501 (2005)
152. P.G. Debenedetti, V.S. Raghavan, S.S. Borick, J. Phys. Chem. **95**, 4540 (1991)
153. V.B. Henriques, M.C. Barbosa, Phys. Rev. E **71**, 031504 (2005)
154. B. Guillot, Y. Guissani, J. Chem. Phys. **119**, 11740 (2003)
155. V.B. Henriques, N. Guisoni, M.A. Barbosa, M. Thielo, M.C. Barbosa, Molec. Phys. **103**, 3001 (2005)
156. A. Barros de Oliveira, G. Franzese, P.A. Netz, M.C. Barbosa, J. Chem. Phys. **128**, 064901 (2008)
157. E.A. Jagla, J. Chem. Phys. **111**, 8980 (1999)
158. T.H. Hall, L. Merril, J.D. Barnett, Science **146**, 1297 (1964)
159. A. Scala, F.W. Starr, E. La Nave, F. Sciortino, H.E. Stanley, Nature **406**, 166 (2000)
160. Z. Yan, S.V. Buldyrev, N. Giovambattista, H.E. Stanley, Phys. Rev. Lett. **95**, 130604 (2005)
161. Z. Yan, S.V. Buldyrev, N. Giovambattista, P.G. Debenedetti, H.E. Stanley, Phys. Rev. E **73**, 051204 (2006)
162. Z. Yan, S.V. Buldyrev, P. Kumar, N. Giovambattista, P.G. Debenedetti, H.E. Stanley, Phys. Rev. E **76**, 051201 (2007)
163. N. Giovambattista, P.J. Rossky, P.G. Debenedetti, Phys. Rev. E **73**, 041604 (2006)
164. C.A. Angell, Ann. Rev. Phys. Chem. **55**, 559 (2004)
165. P.H. Poole, T. Grande, C.A. Angell, P.F. McMillan, Science **275**, 322 (1997)
166. J.L. Yarger, G.H. Wolf, Science **306**, 820 (2004)
167. F. Mallamace, M. Broccio, C. Corsaro, A. Faraone, U. Wanderlingh, L. Liu, C.-Y. Mou, S.-H. Chen, J. Chem. Phys. **124**, 161102 (2006)
168. L. Xu, P. Kumar, S.V. Buldyrev, S.-H. Chen, P.H. Poole, F. Sciortino, H.E. Stanley, PNAS **102**, 16558 (2005)
169. A. Faraone, L. Liu, C.-Y. Mou, C.-W. Yen, S.-H. Chen, J. Chem. Phys. **121**, 10843 (2004)

170. L. Liu, Ph.D. thesis, M.I.T., September 2005
171. J.M.H. Levelt, *Measurements of the Compressibility of Argon in the Gaseous and Liquid Phase*, Ph.D. thesis (University of Amsterdam, Van Gorkum and Co., 1958)
172. M.A. Anisimov, J.V. Sengers, J.M.H. Levelt-Sengers, in *Aqueous System at Elevated Temperatures and Pressures: Physical Chemistry in Water, Stream and Hydrothermal Solutions*, edited by D.A. Palmer, R. Fernandez-Prini, A.H. Harvey (Elsevier, Amsterdam, 2004)
173. M.-C. Bellissent-Funel (ed.), *Hydration Processes in Biology: Theoretical and Experimental Approaches* [Proc. NATO Advanced Study Institutes, Vol. 305] (IOS Press, Amsterdam, 1999)
174. G.W. Robinson, S.-B. Zhu, S. Singh, M.W. Evans, *Water in Biology, Chemistry, and Physics: Experimental Overviews and Computational Methodologies* (World Scientific, Singapore, 1996)
175. C.A. Angell, R.D. Bressel, M. Hemmatti, E.J. Sare, J.C. Tucker, Phys. Chem. Chem. Phys. **2**, 1559 (2000)
176. P.G. Debenedetti, J. Phys.: Cond. Mat. **15**, R1669 (2003)
177. C.A. Angell, J. Phys. Chem. **97**, 6339 (1993)
178. F.W. Starr, C.A. Angell, H.E. Stanley, Physica A **323**, 51 (2003)
179. J. Horbach, W. Kob, Phys. Rev. B **60**, 3169 (1999)
180. E.W. Lang, H.D. Lüdemann, Angew. Chem. Intl. Ed. Engl. **21**, 315 (1982)
181. F.X. Prielmeier, E.W. Lang, R.J. Speedy, H.D. Lüdemann, Phys. Rev. Lett. **59**, 1128 (1987)
182. K. Ito, C.T. Moynihan, C.A. Angell, Nature **398**, 492 (1999)
183. H. Tanaka, J. Phys.: Cond. Mat. **15**, L703 (2003)
184. J. Swenson, H. Jansson, W.S. Howells, S. Longeville, J. Chem. Phys. **122**, 084505 (2005)
185. S. Sastry, C.A. Angell, Nature Mater. **2**, 739 (2003)
186. I. Saika-Voivod, P.H. Poole, F. Sciortino, Nature **412**, 514 (2001)
187. D.C. Rapaport, *The Art of Molecular Dynamics Simulation* (Cambridge University Press, Cambridge, 1995)
188. F.H. Stillinger, A. Rahman, J. Chem. Phys. **57**, 1281 (1972)
189. W. Götze, L. Sjögren, Rep. Prog. Phys. **55**, 241 (1992)
190. P.H. Poole, I. Saika-Voivod, F. Sciortino, J. Phys.: Cond. Mat. **17**, L431 (2005)
191. N. Jakse, L. Hennet, D.L. Price, S. Krishnan, T. Key, E. Artacho, B. Glorieux, A. Pasturel, M.-L. Saboungi, Appl. Phys. Lett. **83**, 4734 (2003)
192. L. Xu, F. Mallamace, F.W. Starr, Z. Yan, S.V. Buldyrev, H.E. Stanley (preprint)
193. P. Kumar, S.V. Buldyrev, S.L. Becker, P.H. Poole, F.W. Starr, H.E. Stanley, PNAS **104**, 9575 (2007)
194. P. Kumar, S.V. Buldyrev, H.E. Stanley (submitted)
195. S.-H. Chen, F. Mallamace, C.-Y. Mou, M. Broccio, C. Corsaro, A. Faraone, PNAS **103**, 12974 (2006)
196. M.G. Mazza, N. Giovambattista, F.W. Starr, H.E. Stanley, Phys. Rev. Lett. **96**, 057803 (2006)
197. M.G. Mazza, N. Giovambattista, H.E. Stanley, F.W. Starr, Phys. Rev. E **76**, 031202 (2007)
198. S.-H. Chen, L. Liu, E. Fratini, P. Baglioni, A. Faraone, E. Mamontov, PNAS **103**, 9012 (2006)
199. F. Mallamace, S.-H. Chen, M. Broccio, C. Corsaro, V. Crupi, D. Majolino, V. Venuti, P. Baglioni, E. Fratini, C. Vannucci, H.E. Stanley, J. Chem. Phys. **127**, 045104 (2007); F. Mallamace, C. Branca, M. Broccio, C. Corsaro, N. Gonzalez-Segredo, H.E. Stanley, S.-H. Chen, Eur. Phys. J. Special Topics **161**, 19 (2008)
200. P. Kumar, F.W. Starr, S.V. Buldyrev, H.E. Stanley, Phys. Rev. E **75**, 011202 (2007)
201. P. Kumar, S.V. Buldyrev, H.E. Stanley, in *Soft Matter under Extreme Pressures: Fundamentals and Emerging Technologies*, edited by S.J. Rzoska, V. Mazur (Springer, Berlin, 2006)
202. D. Liu, Y. Zhang, C.-C. Chen, C.-Y. Mou, P.H. Poole, S.-H. Chen, PNAS **104**, 9570 (2007)
203. D.A. Fuentevilla, M.A. Anisimov, Phys. Rev. Lett. **97**, 195702 (2006)
204. T. Morishita, Phys. Rev. Lett. **97**, 165502 (2006)
205. L. Xu, S.V. Buldyrev, C.A. Angell, H.E. Stanley, Phys. Rev. E **74**, 031108 (2006)
206. F. Mallamace, C. Branca, M. Broccio, C. Corsaro, C.-Y. Mou, S.-H. Chen, PNAS **104**, 18387 (2007)
207. F. Mallamace, C. Corsaro, M. Broccio, C. Branca, N. González-Segredo, J. Spooren, S.-H. Chen, H.E. Stanley (submitted)
208. S.-H. Chen, F. Mallamace, L. Liu, D.Z. Liu, X.Q. Chu, Y. Zhang, C. Kim, A. Faraone, C.-Y. Mou, E. Fratini, P. Baglioni, A.I. Kolesnikov, V. Garcia-Sakai, AIP Conf. Proc. **982**, 39 (2007)
209. S. Maruyama, K. Wakabayashi, M. Oguni, AIP Conf. Proc. **708**, 675 (2004)
210. U. Raviv, P. Laurat, J. Klein, Nature **413**, 51 (2001)
211. S.V. Buldyrev, P. Kumar, P.G. Debenedetti, P. Rossky, H.E. Stanley, PNAS **104**, 20177 (2007)